Polar- and Azimuth-Angle-Dependent Rotational and Vibrational Excitation of Desorbing Product CO_2 in CO Oxidation on Palladium Surfaces

Toshiro Yamanaka* and Tatsuo Matsushima

Catalysis Research Center, Hokkaido University, Sapporo 001-0021, Japan

(Received 2 April 2007; published 17 January 2008)

Clear polar and azimuth angle dependencies were found in rotational and vibrational energies of product CO_2 in CO oxidation on Pd surfaces. On Pd(110)-(1×1), with increases in polar angle, both energies decreased in the [001] direction but remained constant in $[1\bar{1}0]$. On the Pd(110) with missing rows, both energies increased in [001] but decreased in $[1\bar{1}0]$, indicating that the transition state changes with the geometry of the substrate. On Pd(111), the rotational energy greatly increased, but the vibrational energy decreased. Such angular dependence of internal energy provides new dimensions in surface reaction dynamics.

DOI: 10.1103/PhysRevLett.100.026104 PACS numbers: 82.65.+r, 68.35.Ja, 82.20.−w

Elucidation of energy transfer dynamics, transition states (TSs), and their correlation to microscopic structures of substrates is essential to understand surface reactions at the atomic level [1–12], which is required to develop superior catalysts, electrodes, fuel cells, and material growth processes. Angle-resolved (AR) studies on product desorption in surface reactions and on surface scattering processes have provided indispensable information on the dynamics [6–12]. However, compared with information on dynamics in gas-phase reactions, information on dynamics in surface reactions has been limited due to the fast energy relaxation of nascent products [13] and also due to the lack of AR measurements of the internal energy of products, which are necessary to obtain structural information on multidimensional dynamics and TS. In the gas-phase reaction, detailed shapes of the potential energy surface have been evaluated from internal energy since measurements are conducted in AR forms (although angles are usually defined relative to directions of molecular beams) [14]. On the other hand, in the surface reaction, there have been only a few works in which AR measurements of internal (only rotational) energy in photo- and electron-induced desorption were carried out [15–17], and no significant angular dependence was found. For surface thermal reactions, AR measurements of rotational and vibrational energies are still lacking. In this Letter, we describe clear polar and azimuth angle dependencies of vibrational and rotational energies of desorbing product CO_2 characteristic to surface structures in thermal CO oxidation on Pd(110) and Pd(111) surfaces, and we show a new approach to TS structures.

CO oxidation on noble metals has long attracted the attention of chemists, physicists, and also mathematicians due to its practical importance and rich behaviors [1,6,18–26]. It proceeds through adsorption of CO and dissociative adsorption of O_2, diffusion of CO towards an O adatom, formation of a TS (O-CO-metal complex), and then repulsive desorption of CO_2. Recently, structures and energies during formation processes of the TS have been studied in detail by *ab initio* calculations [23–25]. During desorption, the excess energy is partitioned into translational, vibrational, and rotational modes of CO_2. Because of strong repulsion from the surface, desorption of CO_2 is sharply collimated in the direction normal to the CO_2 formation site. As a result, the translational temperature of CO_2 is much higher than the surface temperature (T_{surf}), showing a maximum at the collimation angle [6]. Results of non-AR measurements of infrared emission and absorption showed that rotational and vibrational energies of product CO_2 were also highly excited [18–22].

The design of a new apparatus for analysis of extremely weak infrared emission from AR CO_2 has recently been described in detail [27]. Infrared light emitted in the relaxation of the antisymmetric stretch mode of product CO_2 after passing through two slits for angle selection, $(n_1, n_2, n_3) \rightarrow (n_1, n_2, n_3 - 1)$, where n_1, n_2, and n_3 are the quantum numbers of the symmetric stretch, bending, and antisymmetric stretch modes, respectively, is analyzed by a Fourier-transform infrared spectrometer. The reaction zone at around 1×10^{-3} Torr of the reactants is enclosed in a cylindrical chamber, and the distance from the surface to the first slit is minimized to 4 mm. This pressure was measured by a capacitance manometer at an upper position away from the sample in this reaction chamber. The subsequent path to the second slit at 40 mm from the surface and the emission collector chamber is rapidly evacuated below 10^{-5} and 10^{-7} Torr.

The thin lines in Figs. 1(a)–1(d) show IR emission spectra obtained for Pd(110) at O_2/CO (the ratio of exposure of O_2 to that of CO) $= 1/2$ and $T_{surf} = 600$ K at different desorption polar angles (θ) in the [001] azimuth direction (θ in the x-z plane in the illustration in Fig. 1) at different total reactant pressures (P). In each spectrum, a single broad peak is seen in the range 2400–2200 cm^{-1}, which consists of the contributions from a large number of transition lines corresponding to various initial rovibrational states. According to previous measurements [18–

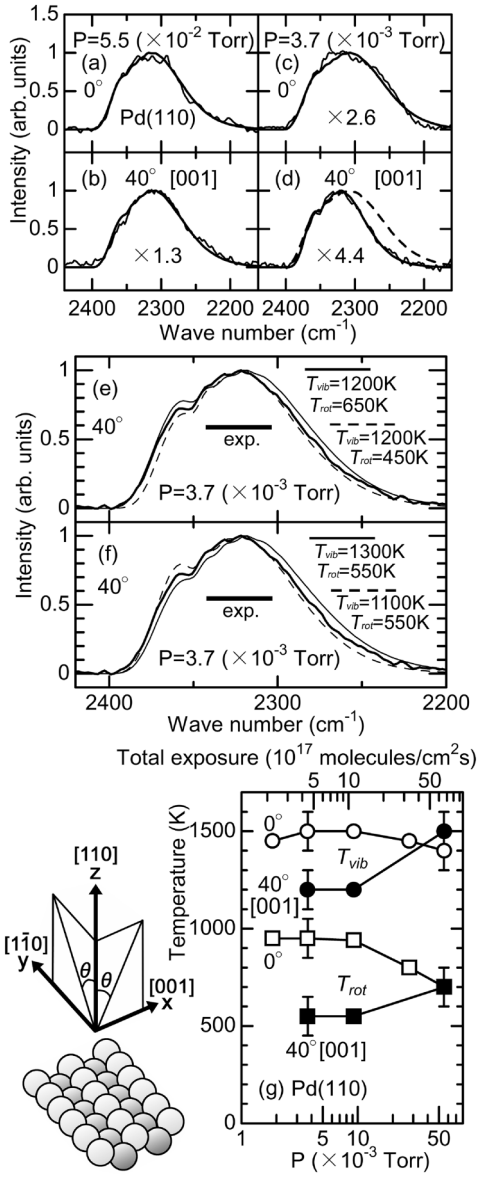

FIG. 1. Chemiluminescence measurements on Pd(110). (a)–(d) Infrared emission spectra at $O_2/CO = 1/2$ and $T_{surf} = 600$ K. The resolution of the wave number is 4 cm^{-1}. Intensities were normalized so that the maxima of peaks become unity. The thin lines show the emission spectra from AR product CO_2 at $\theta = 0°$ and $P = 5.5 \times 10^{-2}$ Torr (a), $\theta = 40°$ in [001] and $P = 5.5 \times 10^{-2}$ Torr (b), $\theta = 0°$ and $P = 3.7 \times 10^{-3}$ Torr (c), and $\theta = 40°$ in [001] and $P = 3.7 \times 10^{-3}$ Torr (d). The thick solid lines show the best results of simulation. These were obtained with $T_{rot} = 700$ K and $T_{vib} = 1400$ K (a), $T_{rot} = 700$ K and $T_{vib} = 1450$ K (b), $T_{rot} = 950$ K and $T_{vib} = 1500$ K (c), and $T_{rot} = 550$ K and $T_{vib} = 1200$ K (d). For comparison, the best simulation at 0° and $P = 3.7 \times 10^{-3}$ Torr is shown by the broken line in (d). (e),(f) Comparison of experimental spectrum (smoothed) and some simulated curves. (g) Dependence on the reactant pressure on Pd(110): T_{vib} at $\theta = 0°$ (open circles), T_{vib} at $\theta = 40°$ ([001]) (closed circles), T_{rot} at $\theta = 0°$ (open squares), and T_{rot} at $\theta = 40°$ ([001]) (closed squares). Total exposure indicates the sum of O_2 exposure and CO exposure and is proportional to P. Schematic illustration of Pd(110), polar angle θ, and azimuthal directions is shown at the bottom of the left side.

22], the populations of vibrational and rotational states of product CO_2 are known to be well expressed by the rotational and vibrational temperatures T_{rot} and T_{vib}, respectively, with corresponding Boltzmann distributions. For the present low-resolution spectra, the position of the broad peak shifts toward lower wave numbers as T_{vib} increases (redshift), whereas the broad spectrum becomes wide at higher T_{rot} values. At $P = 5.5 \times 10^{-2}$ Torr, no meaningful θ dependence was observed, whereas at $P = 3.7 \times 10^{-3}$ Torr, the peak shifted to a higher wave number and the width was reduced as θ increased, indicating lowered T_{vib} and T_{rot}.

The values of T_{rot} and T_{vib} were determined by the curve fitting of the experimentally obtained spectra with simulated ones [18,27]. In our simulation, the line positions presented in the Hitran database [28] were used, and they were linearly extended for transitions from higher rovibrational states. Here, 1487 vibrational bands, each of which contains the transitions from initial rotational states from $J = 0$ to $J = 270$, were taken into account. In the observed spectral window of 2400–2200 cm^{-1}, the contributions of mode 1 (symmetric stretch) and mode 2 (bending) to the redshift are suppressed compared to the contribution of mode 3 (antisymmetric stretch) because mode 3 can contribute through its $\delta n_3 = -1$ transitions, while the $\delta n_2 = -1$ transitions of mode 2 lie outside of the spectral window and the $\delta n_1 = -1$ transitions are inactive for infrared emission. Therefore, from the observed spectrum the temperatures of modes 1 and 2 could not be determined; for this reason it was assumed that all 3 modes have a common temperature T_{vib}, which was then determined as shown in Figs. 1(e) and 1(f). In Fig. 1(e), the width of the simulated curve for $T_{vib} = 1200$ K and $T_{rot} = 450$ K (650 K) is narrower (wider) than experimental results, and in Fig. 1(f), the position of the simulated curve for $T_{vib} = 1100$ K (1300 K) and $T_{rot} = 550$ K lies at higher (lower) wave numbers. Thus, error bars of T_{vib} and T_{rot} are close to 100 K. The thick solid lines in Figs. 1(a)–1(d) show simulated curves for the optimum values of T_{vib} and T_{rot}, i.e., $T_{vib} = 1400$ K and $T_{rot} = 700$ K ($\theta = 0°$, $P = 5.5 \times 10^{-2}$ Torr), 1450 and 700 K (40°, 5.5×10^{-2} Torr), 1500 and 950 K (0°, 3.7×10^{-3} Torr), and 1200 and 550 K (40°, 3.7×10^{-3} Torr). Below 7×10^{-3} Torr, θ dependence of T_{rot} and T_{vib} became independent of P [Fig. 1(g)]. Above this pressure, T_{rot} at $\theta = 0°$ and 40° and T_{vib} at $\theta = 0°$ approach the environmental temperature (600 K) due to scattering with reactants, but T_{vib} at $\theta = 40°$ goes away from 600 K approaching T_{vib} at $\theta = 0°$, indicating slow vibrational relaxation. Both T_{rot} and T_{vib} values became independent of θ. With this apparatus, AR measurements can be performed below 7×10^{-3} Torr, where the mean free path of CO_2 estimated as $\lambda \approx kT/\sqrt{2}\pi\sigma^2 P \approx 20$ mm (σ is the diameter of CO_2 molecule, $T = 600$ K) is sufficiently longer than the distance between the sample and the first slit (4 mm).

θ dependence of T_{rot} and T_{vib} at $O_2/CO = 1/2$ in the x-z plane and the plane in $[1\bar{1}0]$ (y-z plane) is summarized in Fig. 2(a). As θ increased, T_{rot} and T_{vib} clearly decreased in the x-z plane, whereas the values remained constant in the y-z plane. On the other hand, at $O_2/CO = 2$, the anisotropy was reversed [Fig. 2(b)]. As θ increased in the y-z plane, the emission spectra shifted to higher wave numbers, and the width of spectra decreased, indicating lowering of T_{rot} and T_{vib}. In addition, in the x-z plane, the emission spectra shifted to lower wave numbers and the width increased, indicating increased T_{rot} and T_{vib}. For comparison, θ dependence of T_{rot} and T_{vib} on a flat Pd(111) at $O_2/CO = 1/2$, $P = 3.7 \times 10^{-3}$ and $T_{surf} = 700$ K is shown in Fig. 2(c). As θ increases, T_{rot} increases and T_{vib} decreases. T_{rot} at $\theta = 0°$ (350 K) is far below T_{surf}.

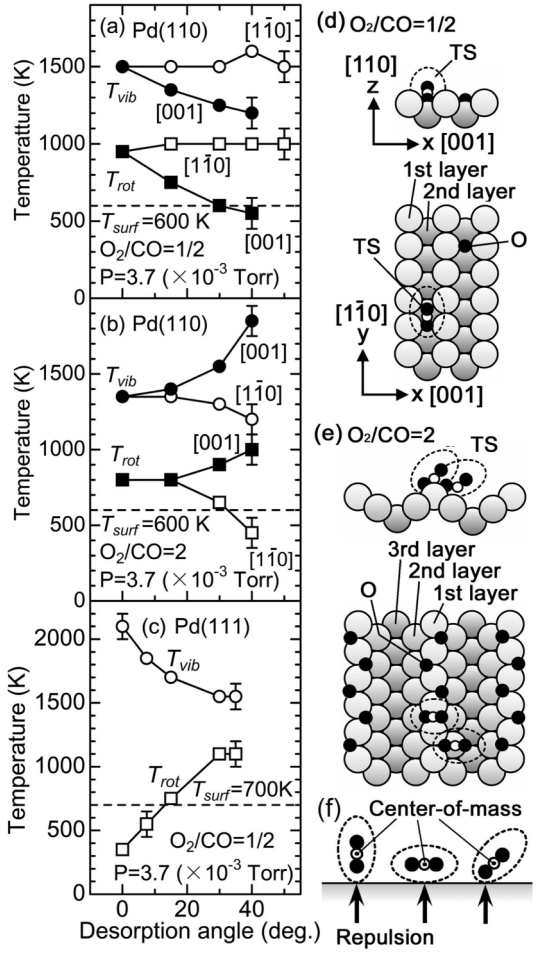

FIG. 2. Angle dependence of the rotational and vibrational temperatures on Pd(110) and Pd(111). (a) Pd(110) at $O_2/CO = 1/2$, $T_{surf} = 600$ K, and $P = 3.7 \times 10^{-3}$ Torr. T_{vib} in $[1\bar{1}0]$ (open circles), T_{vib} in [001] (closed circles), T_{rot} in $[1\bar{1}0]$ (open squares), and T_{rot} in [001] (closed squares). (b) Pd(110) at $O_2/CO = 2$, $T_{surf} = 600$ K, and $P = 3.7 \times 10^{-3}$ Torr. T_{vib} in $[1\bar{1}0]$ (open circles), T_{vib} in [001] (closed circles), T_{rot} in $[1\bar{1}0]$ (open squares), and T_{rot} in [001] (closed squares). (c) Results on Pd(111) at $O_2/CO = 1/2$, $T_{surf} = 700$ K, and $P = 3.7 \times 10^{-3}$ Torr. The open circles and squares show T_{vib} and T_{rot}. (d) Structures of the Pd(110)-(1×1) surface and a proposed TS at $O_2/CO = 1/2$. (e) Structures of Pd(110) with missing rows and a proposed TS at $O_2/CO = 2$. An important point is that TSs are inclined in y-z and x-z planes on Pd(110)-(1×1) and Pd(110) with missing rows, respectively. (f) Three O-C-O TSs with different inclination angles on a flat surface. These are simplified to be linear.

The above results show clear dependence of T_{vib} and T_{rot} of product CO_2 on polar and azimuth angles. Results for Pd(110) at $O_2/CO = 1/2$ (CO_2 yields were the highest) and at $O_2/CO = 2$ (CO_2 yields were reduced to 27%) are quite different. Above 360 K, the (1×1) structure of clean Pd(110) [Fig. 2(d)] is reconstructed into a missing-row structure [i.e., $c(2 \times 4)$-O [Fig. 2(e)]] when the oxygen coverage is high [29,30]. Therefore, the surface structures of Pd(110) at $T_{surf} = 600$ K are thought to be (1×1) and missing-row structures at $O_2/CO = 1/2$ and at $O_2/CO = 2$, respectively. Observed angular dependence of T_{vib} and T_{rot} contains information on structures of surfaces and TS structures on them.

On Pd(110)-(1×1), T_{vib} and T_{rot} in the y-z plane are almost constant and decrease with increases in θ in the x-z plane, as shown in Fig. 2(a). These results indicate that CO_2 with high rovibrational energy can easily move in the y-z plane but that its motion in the x-z plane is hindered. On this surface, CO approaches an oxygen atom at the bottom of the atomic trough [6]. The TS is thought to be inclined in the y-z plane [Fig. 2(d)] and it receives repulsion along the z axis, resulting in rotational motion in the y-z plane. Nascent CO_2 can easily move in the y-z plane, but its motion in the x-z plane is hindered by rows of the 1st Pd layers. As θ increases, the translational temperature and desorption flux of CO_2 decrease gradually in the y-z plane and decrease rapidly in the x-z plane [6], consistent with restricted motions of CO_2 within the y-z plane. If the TS is inclined in the x-z plane, it will receive repulsion in an inclined direction in the x-z plane from both the 1st and 2nd Pd layers. Thus, the restriction of motions within the y-z plane cannot be fully explained by the TS.

On Pd(110) with missing rows, T_{vib} and T_{rot} increased with increase in θ in the x-z plane and decreased in the y-z plane. These results indicate that desorption of CO_2 with high rovibrational energy is promoted at large θ in the x-z plane. On this surface, oxygen atoms form zigzag chains along the y axis near protruding rows of the 1st Pd layer [Fig. 2(e)] [30], and the oxygen at the end of the chain shows high reactivity with CO [31]. Rotational motion in the x-z plane is easy if the TS is inclined in the x-z plane near the protruding row as shown in Fig. 2(e). Also, the motion of nascent CO_2 in the y-z plane may be hindered by neighboring oxygen atoms, although this effect seems less significant. Depending on the position and inclination of the TS, the direction of repulsion from protruding rows may shift from the surface normal in the x-z plane, and also the torque operative to the TS may change. This effect promotes desorption of CO_2 with high rotational energy at large θ in the x-z plane. For CO oxidation on Pt(110) with missing rows, which is similar to the present Pd(110) with

missing rows, a TS inclined in the plane perpendicular to the atomic rows was predicted by *ab initio* calculations [32], consistent with the prediction in this work.

For the TS geometries proposed above, motions of symmetric stretch, bending, and antisymmetric stretch modes are in the y-z plane on Pd(110)-(1×1) and in the x-z plane on Pd(110) with missing rows. The present results show that desorption of CO_2 with high vibrational energy is concentrated in the y-z plane on Pd(110)-(1×1) and in the x-z plane on Pd(110) with missing rows. When TS leaves from the surface becoming CO_2, the excess energy is distributed to translational and vibrational modes. In this process the bent TS [23–25,32] becomes linear and the C-O bond lengths approach that of gas-phase CO_2, resulting in vibrational motions. These structural changes from TS to linear CO_2 may also induce an impulse accelerating the translational motion in the same plane as that of vibration.

Results on flat Pd(111) are different from those on Pd(110)-(1×1) and Pd(110) with missing rows. The enhanced T_{vib} at the surface normal is reasonable because a TS with high energy will receive strong repulsion along the surface normal, inducing sharply collimated desorption of CO_2 with high translational and vibrational energies. The enhanced T_{rot} at large θ can be explained as follows. The repulsion toward the surface normal will excite more translational and less rotational energies if the TS is upright or parallel to the surface [Fig. 2(f)]. On the other hand, more rotational and less translational energy will be excited if the TS is inclined since the repulsion is directed to off-center-of-mass of the TS. Thus, CO_2 with high (low) rotational energy shows a broad (sharp) angular distribution since the angular distribution of desorbing CO_2 with low translational energy is broadened by thermal motions. This effect results in enhanced T_{rot} at large θ. This is consistent with decrease in translational temperature at large θ [6]. It should be noted that D_2 desorbing from Cu(110) with high (low) rotational energy has low (high) translational energy [3,4]. Also, CO_2 may receive repulsion in an off-normal direction when the TS is inclined. This effect can also lead to enhancement of T_{rot} at large θ.

The different angular dependence of internal energies indicates that the orientation of the TS changes with the geometry of substrates when the Pd(110) surface reconstructs. In many reactions, it is difficult to experimentally approach the structures of TSs. The present approach will be applicable to other thermal reactions at a surface and also in gas phase if AR measurements with respect to molecular frame angles are performed using spatially oriented molecules, stimulating further experimental and theoretical works to unveil potential energy surface and multidimensional dynamics.

This research was supported in part by Grant-in-Aid No. 17350002 for General Scientific Research from the Japan Society for the Promotion of Science.

*Corresponding author.
yama@cat.hokudai.ac.jp

[1] R. Imbihl and G. Ertl, Chem. Rev. **95**, 697 (1995).
[2] F. M. Zimmermann and W. Ho, Surf. Sci. Rep. **22**, 127 (1995).
[3] A. Hodgson, Prog. Surf. Sci. **63**, 1 (2000).
[4] H. A. Michelsen, C. T. Rettner, and D. J. Auerbach, Phys. Rev. Lett. **69**, 2678 (1992).
[5] C. T. Rettner and D. J. Auerbach, Phys. Rev. Lett. **74**, 4551 (1995).
[6] T. Matsushima, Surf. Sci. Rep. **22**, 127 (1995).
[7] R. T. Jongma *et al.*, J. Chem. Phys. **107**, 252 (1997).
[8] H. Vach *et al.*, J. Chem. Phys. **100**, 8526 (1994).
[9] F. H. Geuzebroek *et al.*, J. Phys. Chem. **95**, 8409 (1991).
[10] C. T. Rettner and D. J. Auerbach, Science **263**, 365 (1994).
[11] J. W. Elam and D. H. Levy, J. Chem. Phys. **106**, 10 368 (1997).
[12] S. L. Bernasek, M. Zappone, and P. Jiang, Surf. Sci. **272**, 53 (1992).
[13] E. J. Heiweil *et al.*, Annu. Rev. Phys. Chem. **40**, 143 (1989).
[14] R. D. Levine and R. B. Bernstein, *Molecular Reaction Dynamics* (Oxford University Press, New York, 1974).
[15] M. Wilde *et al.*, Surf. Sci. **427–428**, 27 (1999).
[16] A. R. Burns, E. B. Stechei, and D. R. Jennison, Surf. Sci. **280**, 359 (1993).
[17] R. Schwalzwald, A. Modl, and T. J. Chuang, Surf. Sci. **242**, 437 (1991).
[18] D. A. Mantell *et al.*, Surf. Sci. **172**, 281 (1986).
[19] G. W. Coulston and G. L. Haller, J. Chem. Phys. **95**, 6932 (1991).
[20] C. Wei and G. L. Haller, J. Chem. Phys. **103**, 6806 (1995).
[21] D. J. Bald, R. Kunkel, and S. L. Bernasek, J. Chem. Phys. **104**, 7719 (1996).
[22] H. Uetsuka *et al.*, Chem. Lett. **25**, 227 (1996).
[23] A. Alavi *et al.*, Phys. Rev. Lett. **80**, 3650 (1998).
[24] C. J. Zhang and P. Hu, J. Am. Chem. Soc. **123**, 1166 (2001).
[25] P. Salo *et al.*, Surf. Sci. **516**, 247 (2002).
[26] V. P. Zhdanov, Surf. Sci. Rep. **45**, 231 (2002).
[27] T. Yamanaka and T. Matsushima, Rev. Sci. Instrum. **78**, 034105 (2007).
[28] L. S. Rothman *et al.*, J. Quant. Spectrosc. Radiat. Transfer **48**, 537 (1992).
[29] V. R. Dhank *et al.*, Surf. Sci. **260**, L24 (1992).
[30] H. Tanaka, J. Yoshinobu, and M. Kawai, Surf. Sci. **327**, L505 (1995).
[31] W. W. Crew and R. J. Madix, Surf. Sci. **349**, 275 (1996).
[32] T. M. Pedersen, W. X. Li, and B. Hammer, Phys. Chem. Chem. Phys. **8**, 1566 (2006).